Surrogate models to predict maximum dry unit weight, optimum moisture content and California bearing ratio form grain size distribution curve

Saif Alzabeebee
Safaa A. Mohamad
Rwayda Kh. S. Al-Hamd

Alzabeebee , S., Mohamad, S. A., & Al Hamd, R. K. S. (2022). 'Surrogate models to predict maximum dry unit weight, optimum moisture content and California bearing ratio form grain size distribution curve'. *Road Materials and Pavement Design,* 23(12).
DOI: https://doi.org/10.1080/14680629.2021.1995471

Surrogate models to predict maximum dry unit weight, optimum moisture content and California bearing ratio form grain size distribution curve

Saif Alzabeebee (Corresponding author)

Department of Roads and Transport Engineering, College of Engineering, University of Al-Qadisiyah, Al-Qadisiyah, Iraq

E-mail: Saif.Alzabeebee@gmail.com; Saif.Alzabeebee@qu.edu.iq

ORCID iD: https://orcid.org/0000-0001-9685-5641

Safaa A. Mohamad

Highway and Transportation Engineering Department, College of Engineering, Mustansiriyah University, Baghdad, Iraq

E-mail: safaaadnanm@uomustansiriyah.edu.iq

Rwayda Kh. S. Al-Hamd

School of Applied Sciences, Abertay University, Dundee, UK

E-mail: r.al-hamd@abertay.ac.uk

Abstract

This study evaluates the applicability of using a robust, novel, data-driven method in proposing surrogate models to predict the maximum dry unit weight, optimum moisture content, and California bearing ratio of coarse-grained soils using only the results of the grain size distribution analysis. The data-driven analysis has been conducted using evolutionary polynomial regression analysis (MOGA-EPR), employing a comprehensive database. The database included the particle diameter corresponding to a percentage of the passing of 10%, 30%, 50%, and 60%, coefficient of uniformity, coefficient of curvature, dry unit weight, optimum moisture content, and California bearing ratio. The statistical assessment results illustrated that the MOGA-EPR provides robust models to predict the maximum dry unit weight, optimum moisture content, and California bearing ratio. The new models' performance has also been compared with the empirical models proposed by different researchers. It was found from the comparisons that the new models provide enhanced accuracy in predictions as these models scored lower mean absolute error and root mean square error, mean values closer to one, and higher $a20-index$ and coefficient of correlation. Therefore, the new models can be used to ensure more optimized and robust design calculations.

Keywords: maximum dry unit weight; optimum moisture content, California bearing ratio, evolutionary computing, gain size distribution

List of symbols

ANN	The artificial neural network
A	The percentage of amorphous
Ca	The percentage of calcite
C	The percentage of corund
CE	The compaction energy
$D10$	The diameter of the particle corresponding to 10% percentage of passing
$D30$	The diameter of the particle corresponding to 30% percentage of passing
$D50$	The diameter of the particle corresponding to 50% percentage of passing
$D60$	The diameter of the particle corresponding to 60% percentage of passing
e	The void ratio
ELM	The extreme learning machine
$F1.18$	The percentage of passing from sieve with opening of 1.18 mm
$F2.36$	The percentage of passing from sieve with opening of 2.36 mm
$F4.75$	The percentage of passing from sieve with opening of 4.75 mm
$F9.5$	The percentage of passing from sieve with opening of 9.5 mm
$F25$	The percentage of passing from sieve with opening of 25 mm
Fel	The percentage of feldspar
G	The percentage of gravel
GEP	The gene expression programming
GM	The grading modulus
GPR	The Gaussian process regression
Gs	The specific gravity
ID	The relative density
LA	The result of the Los Angeles abrasion test, Q is the percentage of quartz
LL	The liquid limit
LRA	The linear regression analysis
MARC-C	The multivariate adaptive regression splines with piecewise cubic
MLRA	The multiple linear regression analysis
MNLR	The multiple nonlinear regression analysis
MARS-L	The multivariate adaptive regression splines with piecewise linear
$N60$	The corrected result of the standard penetration test
PF	The percentage of fine content
PI	The plasticity index
PL	The plastic limit
PPV	The peak particle velocity
PPV_{2m}	The peak particle velocity at a distance of 2 m from the source
S	The percentage of sand
SL	The shrinkage limit
SVM	The support vector machine
SVR	The support vector regression
WC	The water content
γ_{dry}	The dry density

γ_{dryPL}	The dry density at the plastic limit
$\gamma_{dry\,max}$	The maximum dry density
γ_s	The saturated unit weight of the soil

Introduction

Accurate determination of the maximum dry unit weight, optimum moisture content and California bearing ratio (CBR) is essential for the construction and design of pavements and other highway-related applications. However, the tests required to obtain these parameters are expensive and time-consuming. Therefore, it would be better to have robust predictive models that can be readily used to obtain these parameters. In addition, these models can also be used to double-check the quality of the laboratory tests, serving as an additional quality control check of the accuracy of the tests conducted in the laboratory. Thus, due to the urgent need for tools to predict these parameters, there have been many attempts in the literature to propose models to aid the prediction using linear regression analysis (LRA) (NCHRP, 2001; Gurtug and Sridharan, 2002; Gurtug et al., 2004; Ali et al., 2019; Katte et al., 2019; Gül and Çayir, 2020), multiple linear regression analysis (MLRA) (Reddy and Pavani, 2006; Vinod and Reena, 2008; Breytenbach et al., 2010; Patel and Desai, 2010; Yildirim and Gunaydin, 2011; Ferede, 2012; Alawi and Rajab, 2013; Mujtaba et al., 2013; Patel and Patel, 2013; Ramasubbarao and Siva Sankar, 2013; Talukdar, 2014; Erzin and Turkoz, 2016a, b; Rehman et al., 2017; Saikia et al., 2017; Al-Hamdani, 2018; Farias et al., 2018; Hohn et al., 2022), and soft computing techniques (Yildirim and Gunaydin, 2011; Venkatasubramanian and Dhinakaran, 2011; Kumar et al., 2013; Erzin and Turkoz, 2016a; Kurnaz and Kaya, 2019; Alam et al., 2020). The information collected from previous studies regarding the type of soil employed in the analysis, number of data points, soil parameters employed in the prediction, technique employed in the prediction, and the proposed models (if applicable) are presented in Table 1.

Carefully looking at Table 1, it is clear that majority of past studies have been concerned with the predictions of the optimum moisture content, maximum dry unit weight, and CBR for fine-grained soils. In addition, most of previous studies utilized the percentage of gravel, sand, fine content, and Atterberg limits to aid the prediction of the of the optimum moisture content, maximum dry unit weight, and CBR. However, there have been very few attempts to predict the optimum moisture content, maximum dry unit weight, and CBR using the grain size distribution analysis. In addition, part of previous studies has employed soft computing techniques to predict the aforementioned parameters. However, these previous studies have either proposed complicated models based on limited data or did not propose any model from the artificial intelligence analysis. On the other hand, the models proposed in the literature which correlates the aforementioned parameters with the grain size distribution curve have been proposed using simple regression analyses, although it is widely recognized now that classical regression analyses are not the best solution to develop predictive models due to overfitting issues (Alzabeebee and Chapman, 2020).

Based on the above review, it is clear that there are gaps in knowledge as the previous studies either proposed simple models based on simple regression analysis or complicated models based on artificial intelligence modelling and using limited data. Therefore, the present study aims to employ an extensive database of grain size distribution in an advanced regression analysis aided by a genetic algorithm to provide relatively simple and more robust models to predict the optimum moisture content, maximum dry unit weight and CBR utilizing the results of the grain size distribution for coarse-grained soils.

Table 1: Review of previous studies

No.	Reference	Type of soil	Number of points of the database	Methodology employed in the prediction	Input variables	Output variable	The proposed model/s
1*	NCHRP (2001)	Coarse-grained soils with $PI = 0$	NP	LRA	$D60$	CBR	$CBR = 5$ for $D60 \leq 0.01$ mm $CBR = 28.09\ D60^{0.358}$ for 0.01 mm< $D60 <$ 30 mm $CBR = 95$ for $D60 \geq 30$ mm
2	Gurtug and Sridharan (2002)	Clay	86	LRA	PL	$O.M.C$	$O.M.C = 0.92PL$
3	Gurtug and Sridharan (2002)	Clay	86	LRA	PL	$\gamma_{dry\ max}$	$\gamma_{dry\ max} = 0.98\gamma_{dryPL}$
4*	Gurtug et al. (2004)	Coarse-grained soils	NP	LRA	Cu	$\gamma_{dry\ max}$	$\gamma_{dry\ max} = 13.778\ Cu^{0.166}$
5	Sridharan and Nagaraj (2005)	Fine-grained soils	64	LRA	PL	$O.M.C$	$O.M.C = 0.92PL$
6	Sridharan and Nagaraj (2005)	Fine-grained soils	64	LRA	PL	$\gamma_{dry\ max}$	$\gamma_{dry\ max} = 0.23(93.3 - PL)$
7	Reddy and Pavani (2006)	Fine-grained soils	18	MLRA	PF, LL. and $\gamma_{dry\ max}$	CBR	$CBR = -0.388PF - 0.064LL + 20.38\gamma_{dry\ max}$

8	Sivrikaya et al. (2008)	Fine-grained soils	10	MLRA	PL and CE	$O.M.C$	$O.M.C = PL(1.99 - 0.165 \ln CE)$
9	Sivrikaya et al. (2008)	Fine-grained soils	10	MLRA	$O.M.C$ and CE	$\gamma_{dry\ max}$	$\gamma_{dry\ max} = 14.34 - 0.195 \ln CE - O.M.C(0.073 \ln CE - 0.19)$
10	Vinod and Reena (2008)	NP	NP	MLRA	G, S, and LL	CBR	$CBR = 0.889(LL\left(1 - \frac{S+G}{100}\right)) + 45.616$
11	Breytenbach et al. (2010)	Rocks	60	MLRA	PI and GM	CBR	$CBR = 13{,}984 - 0{,}254PI + 1{,}963GM$
12	Patel and Desai (2010)	Fine-grained soils	12	MLRA	G,S, LL, PL, SL, PI, $O.M.C$, and $\gamma_{dry\ max}$	CBR	$CBR = -0.093PI - 18.78\gamma_{dry\ max} - 0.3081O.M.C + 43.907$
13	Yildirim and Gunaydin (2011)	Fine-grained soils and coarse-grained soils	124	MLRA	G, S, PF, LL, PL, $O.M.C$, and $\gamma_{dry\ max}$	CBR	$CBR = 0.22G + 0.045S + 4.739\gamma_{dry\ max} + 0.122O.M.C$
14	Yildirim and Gunaydin (2011)	Fine-grained soils and coarse-grained soils	124	ANN	G, S, PF, LL, PL, $O.M.C$, and $\gamma_{dry\ max}$	CBR	NP
15	Venkatasubramanian and Dhinakaran (2011)	NP	15	ANN	G, S, PF, LL, PL, PI, $O.M.C$, and $\gamma_{dry\ max}$	CBR	NP
16	Ferede (2012)	Fine-grained soils	27	MLRA	LL, $O.M.C$, and $\gamma_{dry\ max}$	CBR	$CBR = -1.764 - 0.169LL - 0.35O.M.C + 17.965\gamma_{dry\ max}$

17	Alawi and Rajab (2013)	Coarse-grained soils	19	MLRA	G, S, PF, LA, $O.M.C$, and $\gamma_{dry\ max}$	CBR	$CBR = -112.4335 - 0.2856\,LA - 4.7280\,O.M.C + 98.4613\,\gamma_{dry\ max}$
18	Mujtaba et al. (2013)	Sand	110	MLRA	G, S, PF, LL, PI, Gs, Cu, and Cc	$O.M.C$	$\log O.M.C = 1.67 - 0.193 \log Cu - 0.153 \log CE$
19	Mujtaba et al. (2013)	Sand	110	MLRA	G, S, PF, LL, PI, Gs, Cu, and Cc	$\gamma_{dry\ max}$	$\gamma_{dry\ max} = 4.49 \log Cu + 1.15 \log CE + 10.2$
20	Patel and Patel (2013)	Fine-grained soils	29	MLRA	G, S, PF, LL, PL, PI, $O.M.C$, and $\gamma_{dry\ max}$	CBR	$CBR = 2.408\gamma_{dry\ max} - 0.1283O.M.C - 39.345$
21	Ramasubbarao and Siva Sankar (2013)	Fine-grained soils	25	MLRA	G, S, PF, LL, PL, $O.M.C$, and $\gamma_{dry\ max}$	CBR	$CBR = 0.064PF + 0.082S + 0.033G - 0.069LL + 0.157PL - 1.81\gamma_{dry\ max} - 0.061O.M.C$
22	Kumar et al. (2013)	Fine-grained soils and coarse-grained soils	60	ANN	S, PF, LL, PL, PI, $O.M.C$, and $\gamma_{dry\ max}$	CBR	NP
23	Talukdar (2014)	Fine-grained soils	16	MLRA	G, S, PF, LL, PL, PI, $O.M.C$, and $\gamma_{dry\ max}$	CBR	$CBR = 0.127LL + 0.00PL - 0.1598PI + 1.405\gamma_{dry\ max} - 0.259O.M.C + 4.618$
24	Erzin and Turkoz (2016a)	Sand	61	MLRA	G, Cu, Cc, $O.M.C$, $\gamma_{dry\ max}$, Q, Fel, Ca, C, and A	CBR	$CBR = -140.132 - 0.16Q - 0.305Fel - 0.195Ca - 0.436C - 0.45A + 102.192\gamma_{dry\ max} - 6.89G + 49.869Cc - 13.195Cu + 0.844O.M.C$

25	Erzin and Turkoz (2016a)	Sand	61	ANN	G, Cu, Cc, $O.M.C$, $\gamma_{dry\,max}$, Q, Fel, Ca, C, and A	CBR	$CBR = [(0.9 + \tanh W) \times 22.4] + 2.04$, where W is a very complicated model with 10 variables and 31 terms
26	Erzin and Turkoz (2016b)	Sand	NP	MLRA	$O.M.C$, G_s, ID, CC, and Cu	CBR	$CBR = -33{:}229 + 0.3O.M.C + 11.344G_s + 0.618I_D - 21.440C_c + 1.302C_u$
27*	Erzin and Turkoz (2016b)	Sand	NP	MLRA	$O.M.C$, G_s, ID, CC, and Cu	CBR	$CBR = 74.07\gamma_{dry\,max} - 142.23$
28	Farooq et al. (2016)	Fine-grained soils	105	LRA	LL, PL, and CE	$\gamma_{dry\,max}$	$\gamma_{dry\,max} = -0.055LL + 0.014\,PI + 2.21\log(CE) + 12.84$
29	Farooq et al. (2016)	Fine-grained soils	105	LRA	LL, PL, and CE	$O.M.C$	$O.M.C = 0.133LL + 0.02PI - 5.99\log(CE) + 28.60$
30*	Rehman et al. (2017)	Coarse-grained soils	70	MLRA	$D10$, $D30$, $D50$, $D60$, Cc, Cu, Gs, $O.M.C$, and $\gamma_{dry\,max}$	CBR	$CBR = 6.508\,D50 + 1.48\,Cu + 3.97$
31	Saikia et al. (2017)	Fine-grained soils	60	MLRA	LL and PL	$\gamma_{dry\,max}$	$\gamma_{dry\,max} = 21.07 - 0.119LL - 0.02PL$
32	Saikia et al. (2017)	Fine-grained soils	60	MLRA	LL and PL	$O.M.C$	$O.M.C = 0.35LL + 0.163PL + 6.26$
33	Al-Hamdani (2018)	Coarse-grained soils	36	MLRA	G, S, $O.M.C$, Cc, Cu, $D10$, $D30$, $D60$, $F25$, $F9.5$, $F4.75$,	CBR	$CBR = 36.83 + 0.0196F25 - 0.066F9.5 + 0.102F4.75 - 0.0184F2.36 - 0.061F1.18 - 0.180F0.3 - 2.076MDD - 0.141OMC + 0.078G + 0.1141S + 0.13F - 6.335D_{10} - 0.207D_{30} + 0.036D_{60} + 0.012Cc - 0.004Cu$

					$F2.36$, and $F1.18$		
34	Farias et al. (2018)	Fine-grained soils and coarse-grained soils	96	MLRA	G, PF, LL, PL, $O.M.C$, and $\gamma_{dry\ max}$	CBR	$CBR = 0.23 - 0.20F - 0.29LL + 0.40PL$ for $G \leq 35\%$ $CBR = 1.20 - 1.12F - 0.96LL + 1.22PL - 7.33O.M.C$ for $G > 35\%$
35*	Gurtug et al. (2018)	Fine-grained soils and coarse-grained soils	208	LRA	$O.M.C$	$\gamma_{dry\ max}$	$\gamma_{dry\ max} = 51.88\ O.M.C^{-0.4}$
36	Omar et al. (2018)	Fine-grained soils	NP	MLRA, ANN, and SVR	G, S, PF, LL, PL, PI, GS,	$O.M.C$ and $\gamma_{dry\ max}$	NP
37	Ali et al. (2019)	Fine-grained soils	27	LRA	LL and PL	$\gamma_{dry\ max}$	$\gamma_{dry\ max} = 21.5 - 0.1LL$
38	Ali et al. (2019)	Fine-grained soils	27	LRA	LL and PL	$O.M.C$	$O.M.C = 0.31LL + 5$ $O.M.C = 0.56PL + 5.87$
39	Hasnat et al. (2019)	Fine-grained soils	40	MLRA	LL, PL and PI	$O.M.C$	$O.M.C = 0.34LL + 0.17PL$
40	Hasnat et al. (2019)	Fine-grained soils	40	MLRA	LL, PL and PI	$\gamma_{dry\ max}$	$\gamma_{dry\ max} = 21.07 - 0.119LL - 0.02PL$
41	Karimpour-Fard et al. (2019)	Fine-grained soils and coarse-grained soils	728	MLRA	EC, G, S, PF, GS, LL, and PL	$\gamma_{dry\ max}$ and $O.M.C$	NP

42	Karimpour-Fard et al. (2019)	Fine-grained soils and coarse-grained soils	728	ANN	EC, G, S, PF,	$\gamma_{dry\ max}$ and $O.M.C$	NP
43	Katte et al. (2019)	Coarse-grained soils	33	MLRA	G, S, PF, LL, PL, PI, $O.M.C$, and $\gamma_{dry\ max}$	CBR	$CBR = 0.049G - 0.668S - 0.091PL - 0.055PI + 47.13\gamma_{dry\ max} - 2.895O.M.C - 20.19$
44*	Katte et al. (2019)	Coarse-grained soils	33	LRA	G, S, PF, LL, PL, PI, $O.M.C$, and	CBR	$CBR = 99.08 - 5.162\ O.M.C$
45	Kurnaz and Kaya (2019)	Fine-grained soils and coarse-grained soils	158	MLRA	G, S, PF, LL, PI, $O.M.C$, and $\gamma_{dry\ max}$	CBR	$CBR = -2914.5 + 28.948G + 29.064S + 28.812PF + 0.070LL - 0.128PI + 1.574\gamma_{dry\ max} + 0.406O.M.C$
46	Kurnaz and Kaya (2019)	Fine-grained soils and coarse-grained soils	158	ANN	G, S, PF, LL, PI, $O.M.C$, and $\gamma_{dry\ max}$	CBR	NP
47	Alam et al. (2020)	Fine-grained soils	20	GEP	G, S, PF, LL, PL, O.M.C, and $\gamma_{dry\ max}$	CBR	NP
48	Alam et al. (2020)	Fine-grained soils	20	ANN	G, S, PF, LL, PL, O.M.C, and $\gamma_{dry\ max}$	CBR	NP

49	Alam et al. (2020)	Fine-grained soils	20	Krigging method	G, S, PF, LL, PL, $O.M.C$, and $\gamma_{dry\ max}$	CBR	NP
50*	Duque et al. (2020)	Coarse-grained soils	90	MLRA	$D10$, $D30$, $D50$, Cc, Cu	$\gamma_{dry\ max}$	$\gamma_{dry\ max} = 26.75 - 7.1\ D10 + 3.17\ LN(D10) + 0.53\ LN\ (D50)$
51*	Duque et al. (2020)	Coarse-grained soils	90	MLRA	$D10$, $D30$, $D50$, Cc, Cu	$O.M.C$	$O.M.C = 9.92\ D50^{-0.175}Cc^{-0.058}$
52*	Duque et al. (2020)	Coarse-grained soils	90	MLRA	$D10$, $D30$, $D50$, Cc, Cu, $O.M.C$, and $\gamma_{dry\ max}$	CBR	$CBR = 11.03 + 6.61\ D60$
53	Tenpe and Patel (2020a)	Fine-grained soils and coarse-grained soils	389	GEP	G, S, PF, LL, PL, PI, $O.M.C$, and $\gamma_{dry\ max}$	CBR	$CBR = (G - \gamma_{dry\ max}{}^2(PI - 1.142) - O.M.C)^{1/3} - \left(\frac{(LL + S - PF)^{\frac{1}{3}}}{1.6056}\right) + 11.308$
54	Tenpe and Patel (2020a)	Fine-grained soils and coarse-grained soils	389	SVM	G, S, PF, LL, PL, PI, $O.M.C$, and $\gamma_{dry\ max}$	CBR	NP
55	Tenpe and Patel (2020b)	Fine-grained soils and coarse-grained soils	389	ANN	G, S, PF, LL, PL, PI, $O.M.C$, and $\gamma_{dry\ max}$	CBR	NP

56	Gül and Çayir (2020)	Fine-grained soils and coarse-grained soils	21	LRA	WC, γ_{dry}, N60, and PPV	CBR	$CBR = 2.1199N60 - 2.606$ $CBR = -7.3457PPV_{2m} + 116.9$
57	Bardhan et al. (2021a)	Clay, silt and sand	312	ELM and SVM	$G, S, PF, PI, O.M.C$, and $\gamma_{dry\ max}$	CBR	NP
58	Bardhan et al. (2021b)	Clay, silt and sand	312	MARS-L, MARS-C, GPR, and GEP	$G, S, PF, PI, O.M.C$, and $\gamma_{dry\ max}$	CBR	NP
59	Hohn et al. (2022)	Fine-grained soils and coarse-grained soils	169	MNLRA	PF, LL, e, PL, and γ_s	$\gamma_{dry\ max}$	$\gamma_{dry\ max} = 4.1(2.31\gamma_s^{0.5} + 0.27PL^{0.73} + 0.025PF)^{0.72}$
60	Hohn et al. (2022)	Fine-grained soils and coarse-grained soils	169	MNLRA	$PF, LL, PL, PI, O.M.C$, and $\gamma_{dry\ max}$	$O.M.C$	$O.M.C = 0.1LL + 0.07PL^{1.44} + 0.09PF + 2e^{0.27}$

Note: NP means that information has not been clearly illustrated in the original source

Data used in the study

An extensive literature survey has been conducted in this paper to collect a useful and comprehensive database for coarse-grained soils. This resulted in collecting 90 data points from the studies of Rehman et al. (2017) and Duque et al. (2020). Duque et al. (2020) have also used this database to aid the development of his regression models. The collected data are the diameter of the particle equivalent to 10%, 30%, 50%, and 60 percentage of passing in the grain size distribution curve; these parameters have been named as $D10$, $D30$, $D50$ and $D60$. In addition, the coefficient of uniformity (Cu) and coefficient of curvature (Cc), maximum dry unit weight ($\gamma_{dry\ max}$), optimum moisture content ($O.M.C$) and California bearing ratio (CBR) have also been collected. The optimum moisture content and maximum dry unit weight have been determined in accordance with the modified Proctor test as per the ASTM-D1557 (Rehman et al., 2017; Duque et al., 2020). In addition, the CBR test has been conducted for specimen at the optimum moisture content and the maximum dry density as per the modified Procter test. The statistics of the collected database are given in Table 2. Furthermore, the complete data used in the analysis are detailed in a supplementary file with this paper.

It is worthy to state that correlating the grain size distribution characteristics with the optimum moisture content is valid for coarse-grained soils as the grain size distribution controls the void ratio and the latter controls the moisture content (i.e., amount of water that is needed to fill the voids). In addition, all the data used in this study are for specimens that are on the optimum moisture content and subjected to a compaction energy as per the modified Proctor compaction test. Therefore, having the same energy and the optimum moisture content mean also that the grain size distribution control the way the particles packed together due to the applied energy. This means that the grain size distribution also controls the achieved dry unit weight. Furthermore, the stiffness of the packed particles and the friction between the particles control the penetration resistance in the CBR tests, and hence, the grain size distribution also controls the achieved CBR.

Table 2: Statistics of the database employed in this study

Statistical measure	$D10$ (mm)	$D30$ (mm)	$D50$ (mm)	$D60$ (mm)	Cu	Cc	$\gamma_{dry\ max}$ (kN/m^3)	$O.M.C$ (%)	CBR (%)
Minimum	0.07	0.11	0.18	0.20	1.69	0.04	16.29	6.20	6.00
Maximum	0.90	3.00	10.00	14.00	77.78	4.09	21.90	15.40	90.00
Mean	0.21	0.49	1.24	1.70	8.93	0.85	19.63	10.95	22.06
Standard deviation	0.15	0.51	1.68	2.37	13.37	0.56	1.25	2.21	16.69

The implementation of evolutionary polynomial regression analysis (EPR-MOGA)

The novel models developed in this paper to obtain the recompression index are based on a technique called multi-objective genetic algorithm evolutionary polynomial regression analysis (EPR-MOGA) (Giustolisi and Savic, 2006; Giustolisi and Savic, 2009). This technique (i.e., EPR-MOGA) is a novel hybrid intelligent modelling technique that has gained a high reputation in the literature, as it has shown its ability to provide robust models between complex dependent and independent variables (Ahangar Asr et al., 2018; Alzabeebee et al., 2018; Nassr et al., 2018a, b; Alzabeebee et al., 2019; Alzabeebee, 2019; Alzabeebee, 2020a; Alzabeebee, 2020b; Alzabeebee and Chapman, 2020; Shams et al., 2020; Wang et al., 2020). Moreover, the EPR-MOGA technique is considered as a hybrid technique because it combines the regression analysis with artificial intelligence (AI) algorithm (Alzabeebee et al., 2021a, b). The regression analysis is used to aid the process whereas the appropriate constants and exponents of the model under development are optimized by the AI algorithm to give the best fit for the model. The EPR-MOGA modelling involves the following steps:

- The input data sets are prepared for the modelling in the first step, where the data is divided into training data (80%) and validation data (20%).
- The selection of the general mathematical model used to fit the input data is conducted in the second step, where the relationship between the input and output data is assumed for the modelling based on the relevant literature and optimized by trial-and-error process. This step also involves the selection of the exponents range for the mathematical model and the number of terms to be considered for the model.
- The final step involves the implementation EPR-MOGA (regression analysis and AI optimization to provide the model. The developed model is carefully examined using statistical based methodology as will be discussed further in the next section. Based on the obtained statistical performance, the model might be considered appropriate or further optimization is conducted until an excellent prediction accuracy is achieved.

Statistical assessment of the models

The accuracy of the obtained model as well as the previously proposed models is tested by determining the coefficient of correlation (R), mean absolute error (MAE), Root mean square error ($RMSE$), mean (μ), and percentage of predictions within error range of ±20% represented by an index called $a20-index$. These statistical indicators have been calculated using Equations 1 to 4 (Onyejekwe et al., 2015; Zhang and Goh, 2016; Moayedi and Armaghani, 2018; Moayedi and Hayati , 2018; Huang et al., 2019; Wang et al., 2019, 2020; Moayedi et al., 2019a, 2019b, 2020a, 2020b; Liu et al., 2019, 2020; Goh et al., 2020; Nguyen et al., 2020a, 2020b; Zhang et al., 2020).

$$R = \frac{\sum_{i=1}^{n}(Y_{(p)} - Y_{(p)_{average}})(Y_{(m)} - Y_{(m)_{average}})}{\sqrt{\sum_{i=1}^{n}(Y_{(p)} - Y_{(p)_{average}})^2 \sum_{i=1}^{n}(Y_{(m)} - Y_{(m)_{average}})^2}} \tag{1}$$

$$MAE = \frac{1}{n}\sum_{1}^{n}\left|Y_{(p)} - Y_{(m)}\right| \tag{2}$$

$$RMSE = \sqrt{\frac{1}{n}\sum_{1}^{n}\left(Y_{(p)} - Y_{(m)}\right)^2} \tag{3}$$

$$\mu = \frac{1}{n}\sum_{1}^{n}\left(\frac{Y_{(p)}}{Y_{(m)}}\right) \tag{4}$$

$$a20 - index = \frac{Est\ 20}{n} \tag{5}$$

Where, $Y_{(p)}$ is the predicted dependent variable, $Y_{(m)}$ is the measured dependent variable, n is the number of data points used in the calculations, and $Est\ 20$ is the number of estimations within error range of ±20%.

Finally, the performance of the new models is compared against the available empirical models in the literature.

Development of the surrogate models

The database collected from previous studies has been used in the intelligent computing. As mentioned before, the database has been divided into two sets. The first set has been used to train the developed models, while the second set has been used in the model validation stage. Thus, the first set is referred to as the training set, while the second set is named the validation set. Tables 3 and 4 present the statistics of the training and validation data.

Significant efforts have been given to train models to predict the maximum dry unit weight, optimum moisture content, and California bearing ratio with low error and excellent accuracy. These efforts, as has been discussed before, involved checking different exponents range, number of terms, model types and conducting statistical assessments for each produced model.

The best models obtained from the intelligence computing analysis to predict the maximum dry unit weight ($\gamma_{dry\,max}$), optimum moisture content ($O.M.C$), and California bearing ratio (CBR) are shown in Equations 6 to 8, respectively.

$$\begin{aligned}\gamma_{dry\,max} = {} & -0.058\,\frac{D50}{D10\;D60\;Cc} + 0.355\,\frac{D50}{D10\,\sqrt{Cu}\,\sqrt{Cc}} - \frac{2.3}{\sqrt{D10}} \\ & - 0.0384\,\frac{D10}{D30^2\;D60^2\;Cu^2\;Cc^2} - 3.165\,\frac{D10^2}{\sqrt{D50}\,\sqrt{Cc}\;D60} + 25.31\end{aligned} \tag{6}$$

$$\begin{aligned}O.M.C = {} & -0.0000013\,\frac{Cu^2 D60}{Cc^2 D10^2 D50^2 \sqrt{D30}} - 0.052\,\frac{\sqrt{D30}}{D10^2 D60} + \frac{3.92}{\sqrt{D30}\sqrt{D60}} \\ & - 7.245\,\frac{\sqrt{D10}\sqrt{D30}\sqrt{D50}}{D60^2\sqrt{Cc}} + 16.82\,\frac{Cc^2 D10^2}{Cu\;D30\sqrt{D50}} + 6.76\end{aligned} \tag{7}$$

$$\begin{aligned}CBR = {} & 0.0197\,\frac{\sqrt{D50}\sqrt{Cu}\sqrt{Cc}}{D10^2\sqrt{D30}} - 0.06\,\frac{D60^2}{D10} + 16.41\sqrt{D50}\sqrt{D60} \\ & + 14.68\,\frac{\sqrt{D30}}{\sqrt{D60}} - 5.31\,\frac{D50^2\sqrt{D30}}{D60} - 6.2\end{aligned} \tag{8}$$

Figures 1a and b compare the relationship of the MOGA-EPR predictions of $\gamma_{dry\,max}$ (Equation 6) and the corresponding measured values with the no error line and the ±20% error of prediction range for training and validation datasets, respectively. It is evident from the figure that the predictions are close to the no error line for both datasets. Moreover, all of the predictions are within the prediction error range of ±20% for training and validation data, indicating excellent prediction accuracy. Both figures also show that the obtained coefficient of correlation (R) is equal to 0.90 and 0.89 for both training and validation data, respectively. Figures 2a-d show the statistical performance (MAE, $RMSE$, μ, and $a20-index$) of Equation 6 for both training and validation data. The figures illustrate that the model obtained to predict the maximum dry density provides an excellent prediction, where the MAE is very low and is equal to 0.44 and 0.37 for training and validation data, respectively. Also, the obtained $RMSE$ shows that the model does not have issues related to the large error of predictions, where the obtained $RMSE$ is equal to 0.57 and 0.42 for training and validation data, respectively. Furthermore, the obtained mean value is equal to 1.0 (the optimum value) for both datasets. Finally, the $a20-index$ shows that all of the predictions are within the error range of ±20%, which has also been noticed in Figure 1.

The relationship between the MOGA-EPR predictions of the $O.M.C$ (Equation 7) and the corresponding measured values of this important parameter are compared in Figures 3 a and b for both training and validation data, respectively. The figures also present the no error line, lines of prediction error of ±20%, and coefficient of correlation (R). Similar to the previous paragraph's discussion, the accuracy of the predictions is clearly noticeable with the measured-predicted data very close to the no error line. It is also noticeable that almost all of the predictions are within the error range of ±20% for the training dataset, while all of the predictions are within the aforementioned error range (±20%) for the validation data. Figures 3a and b also show that the coefficient of correlation is equal to 0.89 and 0.96 for the training and validation datasets, respectively. Figures 4a-d show the statistical performance of Equation 7, where it is evident that this correlation delivers an excellent accuracy of predictions with MAE, $RMSE$, μ and $a20-index$ of 0.76, 0.98, 1.0 and 0.96, respectively for the training dataset and 0.49, 0.65, 1.0, and 1.0, respectively for the validation dataset.

Similarly, the relationship between the predictions of Equation 8 (the CBR model) with the corresponding measured values are presented in Figures 5a and b, for both the training and validation datasets. Furthermore, the scored MAE, $RMSE$, μ and $a20-index$ of this model are presented in Figures 6a-d for the training and validation dataset. Both figures indicate the excellent accuracy of the developed model with accuracy almost similar to the aforementioned models already discussed in this section.

Table 3: Statistics of the training data

Statistical measure	$D10$ (mm)	$D30$ (mm)	$D50$ (mm)	$D60$ (mm)	Cu	Cc	$\gamma_{dry\ max}$ (kN/m^3)	$O.M.C$ (%)	CBR (%)
Minimum	0.07	0.11	0.18	0.20	1.69	0.04	16.29	6.20	6.00
Maximum	0.90	3.00	10.00	14.00	77.78	4.09	21.90	15.40	90.00
Mean	0.21	0.51	1.33	1.76	9.00	0.88	19.59	10.97	22.69
Standard deviation	0.15	0.55	1.84	2.54	14.18	0.60	1.32	2.21	17.71

Table 4: Statistics of the validation data

Statistical measure	$D10$ (mm)	$D30$ (mm)	$D50$ (mm)	$D60$ (mm)	Cu	Cc	$\gamma_{dry\ max}$ (kN/m^3)	$O.M.C$ (%)	CBR (%)
Minimum	0.12	0.18	0.20	0.27	2.06	0.25	18.10	6.70	7.00
Maximum	0.70	1.10	2.10	5.10	36.43	1.08	21.50	14.50	43.00
Mean	0.21	0.40	0.89	1.44	8.64	0.72	19.82	10.88	19.50
Standard deviation	0.13	0.27	0.69	1.48	9.84	0.31	0.96	2.29	11.79

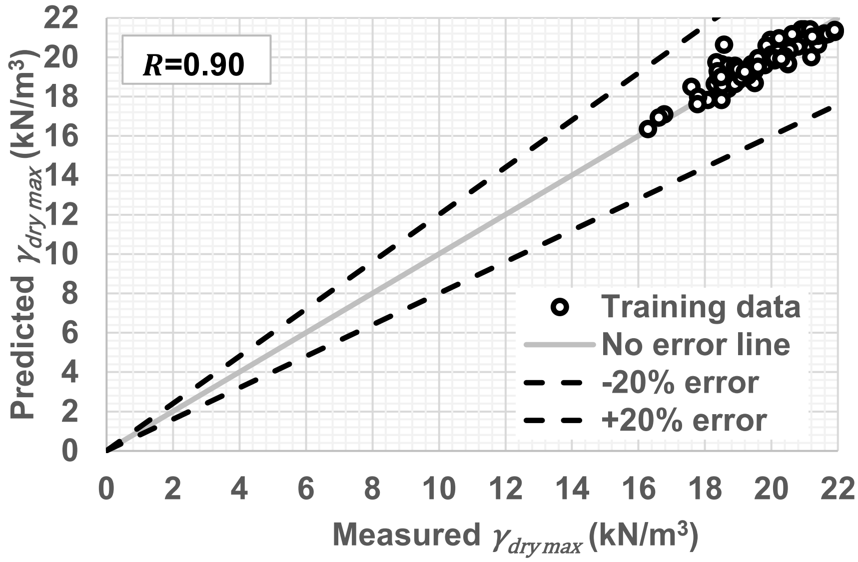

(a) Training data

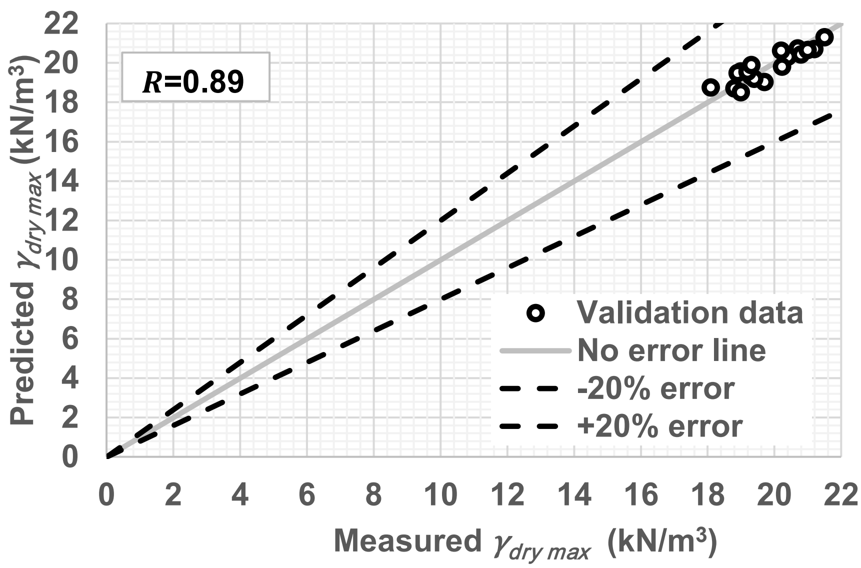

(b) Validation data

Figure 1: Comparison of the measured and hybrid prediction of the maximum dry unit weight (Equation 6)

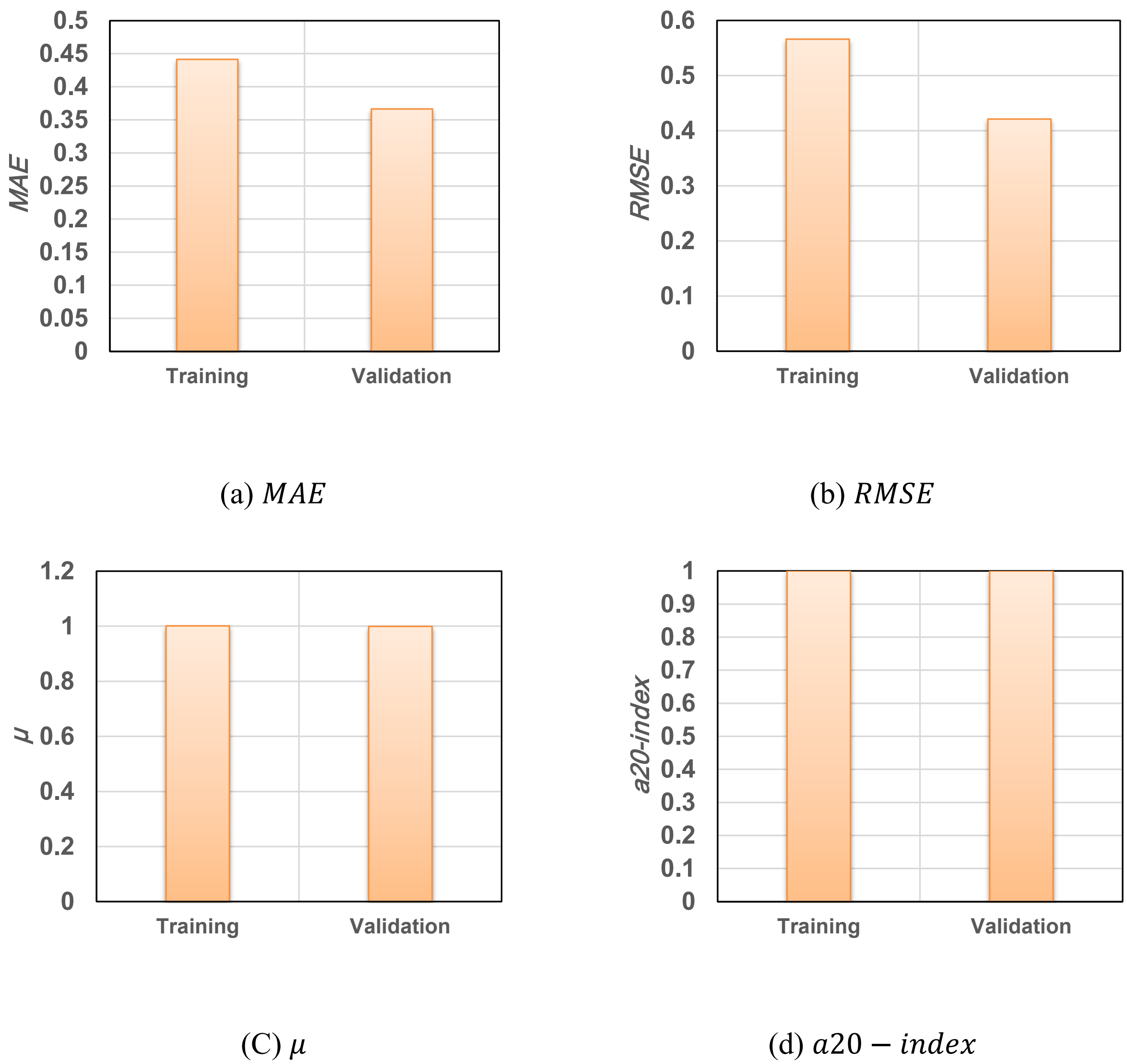

(a) MAE

(b) $RMSE$

(C) μ

(d) $a20 - index$

Figure 2: Statistical performance of the surrogate model to predict the maximum dry unit weight of the soil (Equation 6)

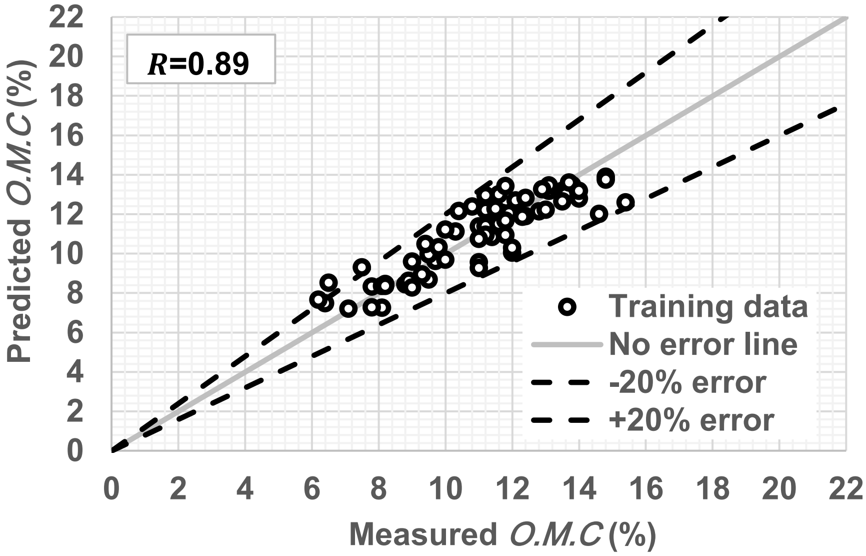

(a) Training data

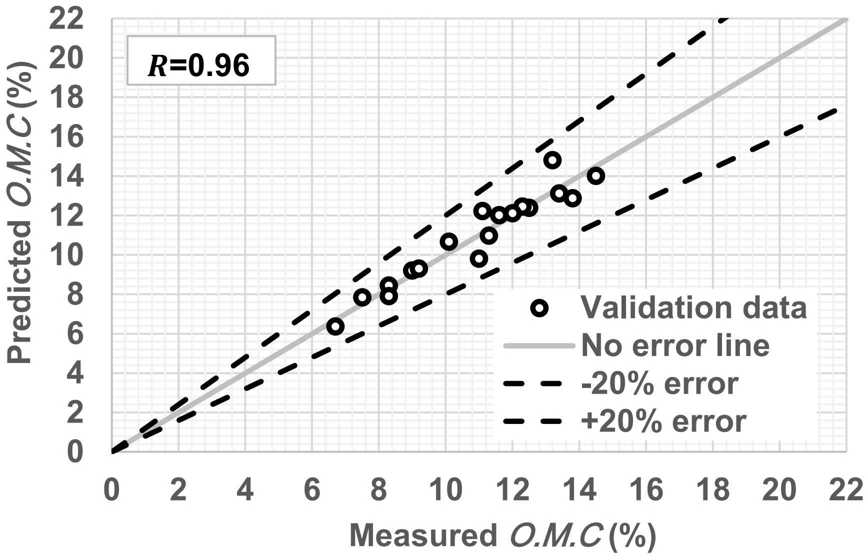

(b) Validation data

Figure 3: Comparison of the measured and hybrid prediction of the optimum moisture content (Equation 7)

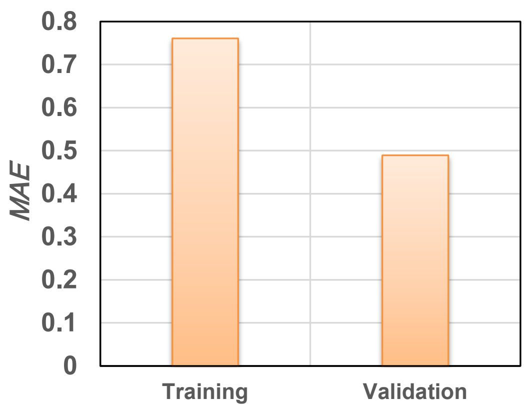

(a) MAE

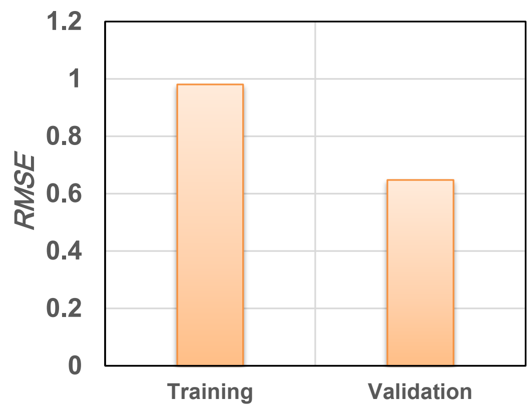

(b) $RMSE$

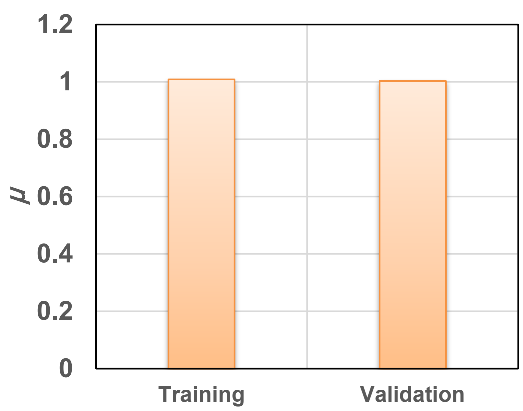

(C) μ

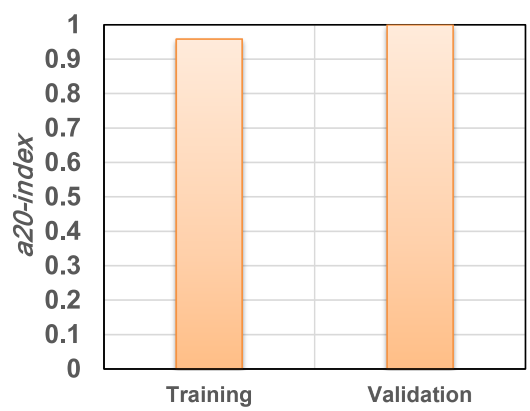

(d) $a20 - index$

Figure 4: Statistical performance of the surrogate model to predict the optimum moisture content of the soil (Equation 7)

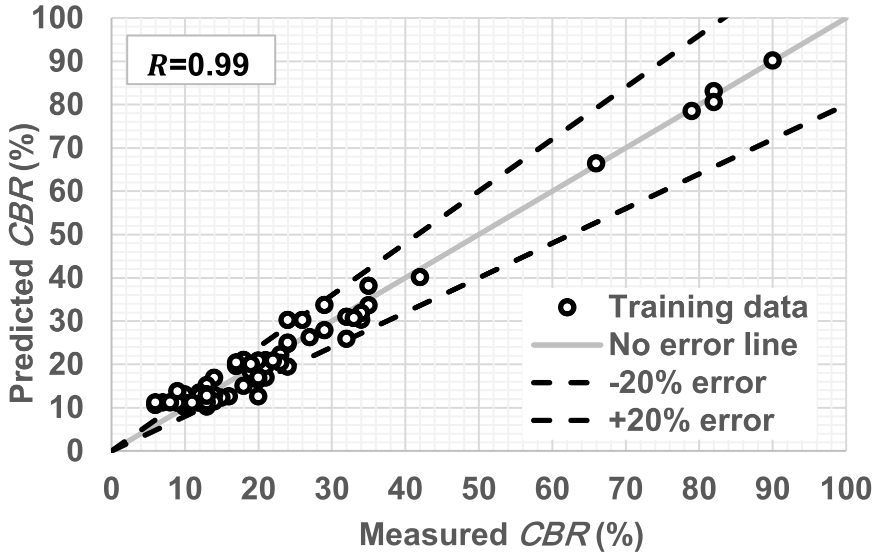

(a) Training data

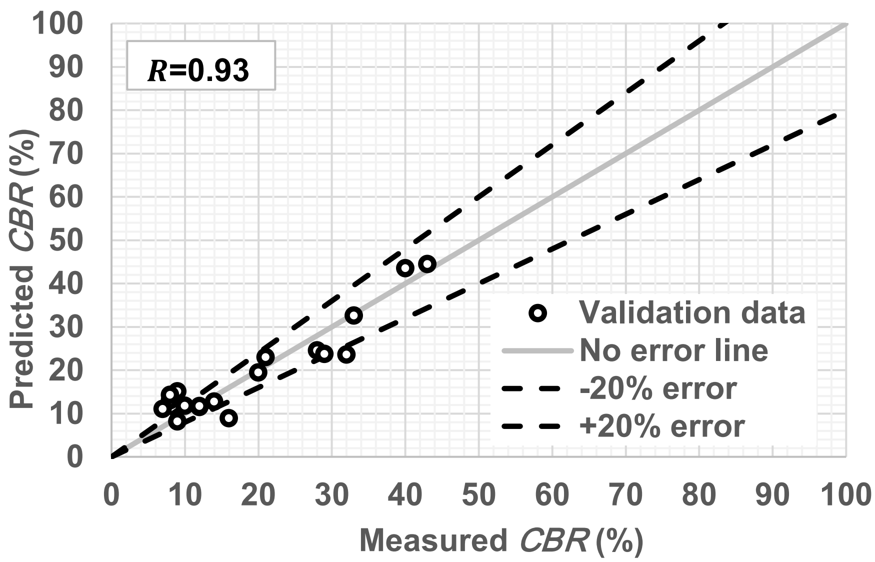

(b) Validation data

Figure 5: Comparison of the measured and hybrid prediction of the California bearing ratio (Equation 8)

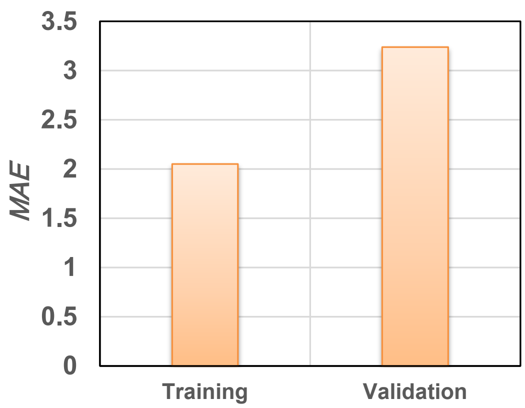

(a) MAE

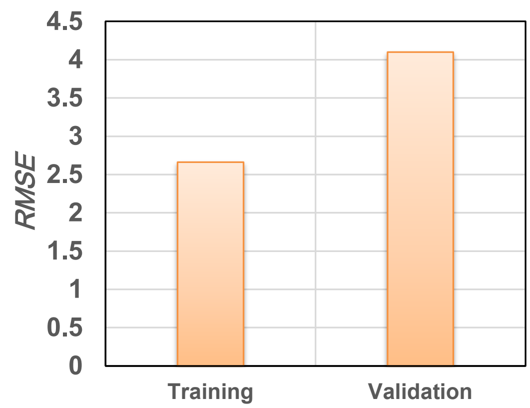

(b) $RMSE$

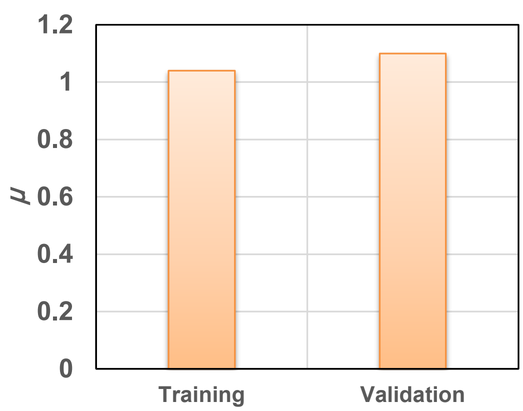

(C) μ

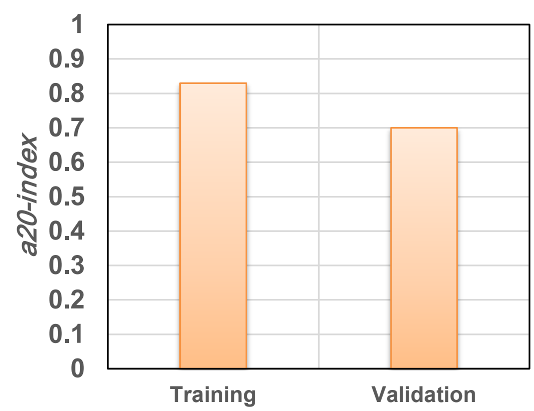

(d) $a20 - index$

Figure 6: Statistical performance of the surrogate model to predict the California bearing ratio of the soil (Equation 8)

Comparison of the new models with previous empirical models

The performance of the developed models has been compared with those available in the literature which have been developed for coarse-grained soils and employing the same parameters collected in this research (i.e., $D10$, $D30$, $D50$, $D60$, Cu, Cc, $\gamma_{dry\ max}$, $O.M.C$, and CBR); these models are donated with * in Table 1. These models available in the literature are already presented in Table 1 and discussed in the introduction section. The comparisons are also based on the statistical performance (i.e., the obtained MAE, $RMSE$, μ, $a20-index$, and R).

Tables 5 compares the statistical performance of Equation 6 with the models presented in Table 1 (Gurtug et al., 2004; Gurtug et al., 2018; Duque et al., 2020). The training and validation datasets have been kept separated in this comparison to provide more accurate comparisons. The scored values presented in the table undoubtedly show that the new developed model is more accurate than previous models as this model scored lower error for both datasets, slightly higher mean for the validation dataset, and higher coefficient of correlation for both datasets. It is also clear from the table that the model proposed by Duque et al. (2020) is more accurate than the model developed by Gurtug et al. (2004) and Gurtug et al. (2018), where Gurtug et al. (2004) model scored very low coefficient of correlation and did not predict any point within error range of ±20% and the model of Gurtug et al. (2018) scored lower coefficient of correlation for both dataset, higher error for both dataset, and lower a20-index for the validation data compared with the new model.

Table 6 assesses the performance of Equation 7 against the model proposed by Duque et al. (2020) to predict the optimum moisture content. The scored statistical indicators also demonstrate that the new model is better than the available one, and for both datasets. The main significant difference in both models is that the new models scored much less MAE and $RMSE$ for the validation dataset. In addition, the $a20-index$ values show that the new model provides 100% predictions within an error range of ±20% for the validation dataset, while Duque et al. (2020) model only predicted 56% of the data within this error range. Furthermore, the new model also provides a lower error, higher $a20-index$, and higher coefficient of correlation for the training dataset compared with Duque et al. (2020) model.

Finally, Table 7 compares the performance of Equation 8 (the new model to predict the California bearing ratio) with the previous empirical models. The new model shows better performance for both datasets with a lower error, mean closer to the optimum value, higher percentage of predictions within an error range of ±20% and higher coefficient of correlation. Duque et al. (2020) model also scored good performance for the training dataset. However, this model only predicted 11% of the validation data within an error range of 20%, although the scored coefficient of correlation was remarkably high (0.90), and the obtained mean value was also close to the optimum value. This indicates that the coefficient of correlation and the mean cannot be used alone to judge a model's accuracy. Overall, Katte et al. (2019) model provides the poorest prediction for both datasets with MAE, $RMSE$, μ, $a20-index$, and R equal to 22.18, 23.29, 2.38, 0.03, and 0.72, respectively for the training dataset and 23.53, 28.22, 2.6, 0.22, and 0.87, respectively for the validation dataset.

Table 5: Comparison of the developed model and the previous empirical models to predict the maximum dry unit weight

Dry unit weight model	Data set	MAE	$RMSE$	μ	$a20-index$	R
Present study (Equation 6)	Training data	0.44	0.57	1.00	1.00	0.90
Gurtug et al. (2004)		9.09	9.38	0.54	0.00	0.50
Gurtug et al. (2018)		1.21	1.54	1.03	1.00	0.6
Duque et al. (2020)		0.59	0.72	1.00	1.00	0.84

Present study (Equation 6)	Validation data	0.37	0.42	1.00	1.00	0.89
Gurtug et al. (2004)		9.84	9.98	0.51	0.00	0.41
Gurtug et al. (2018)		1.74	2.21	1.01	0.94	0.59
Duque et al. (2020)		1.34	1.63	0.98	1.00	0.89

Table 6: Comparison of the developed model and the previous empirical models to predict the optimum moisture content

$O.M.C$ model	Data set	MAE	$RMSE$	μ	$a20-index$	R
Present study (Equation 7)	Training data	0.76	0.98	1.01	0.96	0.89
Duque et al. (2020)		0.96	1.21	1.00	0.92	0.84
Present study (Equation 7)	Validation data	0.49	0.65	1.00	1.00	0.96
Duque et al. (2020)		2.32	2.92	1.14	0.56	0.91

Table 7: Comparison of the developed model and the previous empirical models to predict the California bearing ratio

California bearing ratio	Data set	MAE	$RMSE$	μ	$a20-index$	R
Present study (Equation 8)	Training data	2.05	2.66	1.04	0.83	0.99
Duque et al. (2020)		3.26	4.46	1.09	0.75	0.97
Rehman et al. (2017)		7.53	16.88	1.04	0.39	0.95
Katte et al. (2019)		22.18	23.29	2.38	0.03	0.72

NCHRP (2001)		9.38	10.36	1.57	0.17	0.94
Present study (Equation 8)		3.24	4.10	1.10	0.70	0.93
Duque et al. (2020)		14.62	20.79	1.30	0.11	0.90
Rehman et al. (2017)	Validation data	17.37	26.17	1.43	0.22	0.87
Katte et al. (2019)		23.53	28.22	2.68	0.22	0.87
NCHRP (2001)		15.57	21.14	1.82	0.28	0.92

Conclusions

In this paper, the MOGA-EPR technique was used to developed accurate models to predict the maximum dry unit weight, optimum moisture content, and California bearing ratio of coarse-grained soils based on the results obtained from grain size distribution analysis. In addition, the developed models have been compared with those available in the literature using statistical performance parameters (mean absolute error (MAE), root mean square error ($RMSE$), mean (μ), $a20-index$, and coefficient of correlation (R)). the following conclusions can be drawn:

1- The model proposed in this paper to predict the maximum dry unit weight (Equation 6) shows more reliable predications compared with the models proposed in the literature. The MAE, $RMSE$, μ, $a20-index$ and R for this model are 0.44, 0.57, 1.00, 1.00 ad 0.90, respectively for the training dataset and 0.37, 0.42, 1.00, 1.00 and 0.89, respectively for the validation dataset (see Table 5 for detailed comparison).

2- The model proposed in this paper to predict the optimum moisture contains prediction (Equation 7) demonstrated better predictions than the model proposed by Duque et al. (2020). This model scored MAE, $RMSE$, μ, $a20-index$ and R of 0.76, 0.98, 1.01, 0.96, and 0.89, respectively for the training dataset and 0.49, 0.65, 1.00, 1.00 and 0.96, respectively for the validation dataset (see Table 6 for detailed comparison).

3- The third model proposed in this paper showed an enhanced prediction accuracy for the California bearing ratio (Equation 8) compared with the model proposed in the literature. The scored MAE, $RMSE$, μ, $a20-index$ and R for this model are 2.05, 2.66, 1.04, 0.83 and 0.99, respectively for the training dataset and 3.24, 4.10, 1.10, 0.70 and 0.93, respectively for validation dataset (see Table 7 for detailed comparison).

Lastly, this study has shown a coherent methodology to adopt a well-established novel AI algorithm implementation to develop simple and accurate models to predict three of the most needed parameters in the pavement design. In addition, the results demonstrated the accuracy of these models compared with the previously proposed empirical models. Hence, the proposed models can enhance the designs by reducing the time required to obtain the parameters and thus, save some costs of projects. Also, these models can also be used for experimental validation if there is a budget and time to do the compaction and CBR tests.

References

Ahangar Asr, A., Faramarzi, A. and Javadi, A.A. (2018). An evolutionary modelling approach to predicting stress-strain behaviour of saturated granular soils, Engineering Computations, Vol. 35 No. 8, pp. 2931-2952. https://doi.org/10.1108/EC-01-2018-0025

Alam, S.K., Mondal, A. and Shiuly, A., 2020. Prediction of CBR value of fine grained soils of Bengal Basin by genetic expression programming, artificial neural network and krigging method. Journal of the Geological Society of India, 95(2), pp.190-196.

Alawi, M. and Rajab, M., 2013. Prediction of California bearing ratio of subbase layer using multiple linear regression models. Road materials and pavement design, 14(1), pp.211-219.

Al-Hamdani, D.A., 2018. Correlation of Cbr Value With Particles Size and Compaction Characteristics of Cohesionless Soil. Kufa Journal of Engineering, 9(1).

Ali, H.F.H., Rash, A.J.H. and Muhedin, D.A., 2019. A Correlation between Compaction Characteristics and Soil Index Properties for Fine-grained Soils. Polytechnic Journal, 9(2), pp.93-99.

Alzabeebee, S. and Chapman, D.N., 2020. Evolutionary computing to determine the skin friction capacity of piles embedded in clay and evaluation of the available analytical methods. Transportation Geotechnics, p.100372.

Alzabeebee, S., 2019. Seismic response and design of buried concrete pipes subjected to soil loads. Tunnelling and Underground Space Technology, 93, 103084.

Alzabeebee, S., 2020a. Application of EPR-MOGA in computing the liquefaction-induced settlement of a building subjected to seismic shake. Engineering with Computers, https://doi.org/10.1007/s00366-020-01159-9

Alzabeebee, S., 2020b. Dynamic response and design of a skirted strip foundation subjected to vertical vibration. Geomechanics and Engineering, 20(4), pp.345-358.

Alzabeebee, S., Alshkane, Y.M. and Rashed, K.A., 2021. Evolutionary computing of the compression index of fine-grained soils. Arabian Journal of Geosciences, 14(19), pp.1-17.

Alzabeebee, S., Alshkane, Y.M., Al-Taie, A.J. and Rashed, K.A., 2021. Soft computing of the recompression index of fine-grained soils. Soft Computing, https://doi.org/10.1007/s00500-021-06123-3

Alzabeebee, S., Chapman, D.N. and Faramarzi, A., 2018. Development of a novel model to estimate bedding factors to ensure the economic and robust design of rigid pipes under soil loads. Tunnelling and Underground Space Technology, 71, pp.567-578.

Alzabeebee, S., Chapman, D.N. and Faramarzi, A., 2019. Economical design of buried concrete pipes subjected to UK standard traffic loading. Proceedings of the Institution of Civil Engineers-Structures and Buildings, 172(2), pp.141-156.

Bardhan, A., Gokceoglu, C., Burman, A., Samui, P. and Asteris, P.G., 2021b. Efficient computational techniques for predicting the California bearing ratio of soil in soaked conditions. Engineering Geology, p.106239.

Bardhan, A., Samui, P., Ghosh, K., Gandomi, A.H. and Bhattacharyya, S., 2021a. ELM-based adaptive neuro swarm intelligence techniques for predicting the California bearing ratio of soils in soaked conditions. Applied Soft Computing, p.107595.

Breytenbach, I.J., Paige-Green, P. and Van Rooy, J.L., 2010. The relationship between index testing and California Bearing Ratio values for natural road construction materials in South Africa. Journal of the South African Institution of Civil Engineering, 52(2), pp.65-69.

Duque, J., Fuentes, W., Rey, S. and Molina, E., 2020. Effect of grain size distribution on California bearing ratio (CBR) and modified proctor parameters for granular materials. Arabian Journal for Science and Engineering, 45, pp.8231-8239.

Erzin, Y. and Turkoz, D., 2016a. Use of neural networks for the prediction of the CBR value of some Aegean sands. Neural Computing and Applications, 27(5), pp.1415-1426.

Erzin, Y., Tuskan, Y., Turkoz, D. and Yılmaz, I., 2016. Investigations on factors influencing the CBR value of some Aegean sands. Scientia Iranica, 23(2), pp.420-428.

Farias, I.G., Araujo, W. and Ruiz, G., 2018. Prediction of California bearing ratio from index properties of soils using parametric and non-parametric models. Geotechnical and Geological Engineering, 36(6), pp.3485-3498.

Farooq, K., Khalid, U. and Mujtaba, H., 2016. Prediction of compaction characteristics of fine-grained soils using consistency limits. Arabian Journal for science and Engineering, 41(4), pp.1319-1328.

Ferede, Z.W., 2012. Prediction of California Bearing Ratio (CBR) value from Index Properties of Soil. M.Sc. dissertation, Addis Ababa Institute of Technology.

Giustolisi, O. and Savic, D.A., 2006. A symbolic data-driven technique based on evolutionary polynomial regression. Journal of Hydroinformatics, 8(3), pp.207-222.

Giustolisi, O. and Savic, D.A., 2009. A symbolic data-driven technique based on evolutionary polynomial regression. Journal of Hydroinformatics, 8(3), pp.207-222.

Goh, A.T.C., Zhang, R.H., Wang, W., Wang, L., Liu, H.L. and Zhang, W.G., 2020. Numerical study of the effects of groundwater drawdown on ground settlement for excavation in residual soils. Acta Geotechnica, 15(5), pp.1259-1272.

Gül, Y. and Çayir, H.M., 2020. Prediction of the California bearing ratio from some field measurements of soils. Proceedings of the Institution of Civil Engineers-Municipal Engineer, https://doi.org/10.1680/jmuen.19.00020

Gurtug, Y. and Sridharan, A., 2002. Prediction of compaction characteristics of fine-grained soils. Geotechnique, 52(10), pp.761-763.

Gurtug, Y. and Sridharan, A., 2004. Compaction behaviour and prediction of its characteristics of fine grained soils with particular reference to compaction energy. Soils and Foundations, 44(5), pp.27-36.

Gurtug, Y., Sridharan, A. and Ikizler, S.B., 2018. Simplified method to predict compaction curves and characteristics of soils. Iranian Journal Of Science and Technology, Transactions Of Civil Engineering, 42(3), pp.207-216.

Hasnat, A., Hasan, M.M., Islam, M.R. and Alim, M.A., 2019. Prediction of Compaction Parameters of Soil using Support Vector Regression. Current Trends in Civil and Structural Engineering, 4(1), 1-7.

Hassanlourad, M., Ardakani, A., Kordnaeij, A. and Mola-Abasi, H., 2017. Dry unit weight of compacted soils prediction using GMDH-type neural network. The European Physical Journal Plus, 132(8), p.357.

Hohn, A. V., Leme, R. F., da Silva Filho, F. C., Moura, T. E., and Llanque, G. R. A. (2022). Empirical Models to Predict Compaction Parameters for Soils in the State of Ceará, Northeastern Brazil. Ingeniería e Investigación, 42(1), e86328. https://doi.org/10.15446/ing.investig.v42n1.86328

Hossein Alavi, A., Hossein Gandomi, A., Mollahassani, A., Akbar Heshmati, A. and Rashed, A., 2010. Modeling of maximum dry density and optimum moisture content of stabilized soil using artificial neural networks. Journal of Plant Nutrition and Soil Science, 173(3), pp.368-379.

Huang, C.F., Li, Q., Wu, S.C., Liu, Y. and Li, J.Y., 2019. Assessment of empirical equations of the compression index of muddy clay: sensitivity to geographic locality. Arabian Journal of Geosciences, 12(4), 122. https://doi.org/10.1007/s12517-019-4276-5

Karimpour-Fard, M., Machado, S.L., Falamaki, A., Carvalho, M.F. and Tizpa, P., 2019. Prediction of compaction characteristics of soils from index test's results. Iranian Journal of Science and Technology, Transactions of Civil Engineering, 43(1), pp.231-248.

Katte, V.Y., Mfoyet, S.M., Manefouet, B., Wouatong, A.S.L. and Bezeng, L.A., 2019. Correlation of California bearing ratio (CBR) value with soil properties of road subgrade soil. Geotechnical and Geological Engineering, 37(1), pp.217-234.

Kumar, S.A., Kumar, J.P. and Rajeev, J., 2013. Application of machine learning techniques to predict soaked CBR of remolded soils. International Journal of Engineering Research and Technology, 2(6), 3019-3024.

Kurnaz, T.F. and Kaya, Y., 2019. Prediction of the California bearing ratio (CBR) of compacted soils by using GMDH-type neural network. The European Physical Journal Plus, 134(7), p.326.

Liu, L., Moayedi, H., Rashid, A.S.A., Rahman, S.S.A. and Nguyen, H., 2020. Optimizing an ANN correlation with genetic algorithm (GA) predicting load-settlement behaviours of eco-friendly raft-pile foundation (ERP) system. Engineering with Computers, 36(1), pp.421-433.

Liu, W., Moayedi, H., Nguyen, H., Lyu, Z. and Bui, D.T., 2019. Proposing two new metaheuristic algorithms of ALO-MLP and SHO-MLP in predicting bearing capacity of circular footing located on horizontal multilayer soil. Engineering with Computers, DOI: https://doi.org/10.1007/s00366-019-00897-9

Moayedi, H. and Armaghani, D.J., 2018. Optimizing an ANN correlation with ICA for estimating bearing capacity of driven pile in cohesionless soil. Engineering with Computers, 34(2), pp.347-356.

Moayedi, H. and Hayati, S., 2018. Correlationling and optimization of ultimate bearing capacity of strip footing near a slope by soft computing methods. Applied Soft Computing, 66, 208-219.

Moayedi, H., Mehrabi, M., Mosallanezhad, M., Rashid, A.S.A. and Pradhan, B., 2019a. Modification of landslide susceptibility mapping using optimized PSO-ANN technique. Engineering with Computers, 35(3), pp.967-984.

Moayedi, H., Moatamediyan, A., Nguyen, H., Bui, X.N., Bui, D.T. and Rashid, A.S.A., 2020b. Prediction of ultimate bearing capacity through various novel evolutionary and neural network correlations. Engineering with Computers, 36, 671-687.

Moayedi, H., Nguyen, H. and Rashid, A.S.A., 2019b. Comparison of dragonfly algorithm and Harris hawks optimization evolutionary data mining techniques for the assessment of bearing capacity of footings over two-layer foundation soils. Engineering with Computers, DOI: https://doi.org/10.1007/s00366-019-00834-w

Moayedi, H., Raftari, M., Sharifi, A., Jusoh, W.A.W. and Rashid, A.S.A., 2020a. Optimization of ANFIS with GA and PSO estimating α ratio in driven piles. Engineering with Computers, 36(1), pp.227-238.

Mujtaba, H., Farooq, K., Sivakugan, N. and Das, B.M., 2013. Correlation between gradational parameters and compaction characteristics of sandy soils. International Journal of Geotechnical Engineering, 7(4), pp.395-401.

Nassr, A., Esmaeili-Falak, M., Katebi, H. and Javadi, A., 2018a. A new approach to modeling the behavior of frozen soils. Engineering Geology, 246, pp.82-90.

Nassr, A., Javadi, A. and Faramarzi, A., 2018b. Developing constitutive models from EPR-based self-learning finite element analysis. International Journal for Numerical and Analytical Methods in Geomechanics, 42(3), pp.401-417.

NCHRP.: Correlation of CBR values with soil index guide for mechanistic and empirical-design for new a rehabilitated pavement structures, Illinois (2001)

Nguyen, H., Moayedi, H., Foong, L.K., Al Najjar, H.A.H., Jusoh, W.A.W., Rashid, A.S.A. and Jamali, J., 2020b. Optimizing ANN correlations with PSO for predicting short building seismic response. Engineering with Computers, 36,823–837.

Nguyen, H., Moayedi, H., Jusoh, W.A.W. and Sharifi, A., 2020a. Proposing a novel predictive technique using M5Rules-PSO correlation estimating cooling load in energy-efficient building system. Engineering with Computers, 36, 857-7866.

Omar, M., Shanableh, A., Mughieda, O., Arab, M., Zeiada, W. and Al-Ruzouq, R., 2018. Advanced mathematical models and their comparison to predict compaction properties of fine-grained soils from various physical properties. Soils and Foundations, 58(6), pp.1383-1399.

Onyejekwe, S., Kang, X. and Ge, L., 2015. Assessment of empirical equations for the compression index of fine-grained soils in Missouri. Bulletin of Engineering Geology and the Environment, 74(3), pp.705-716.

Patel, M.A and Patel, H.S., 2013. Laboratory assessment to correlate strength parameter from physical properties of subgrade. Procedia Engineering, 51, pp.200-209.

Patel, R.S. and Desai, M.D., 2010, December. CBR predicted by index properties for alluvial soils of South Gujarat. In Proceedings of the Indian geotechnical conference, Mumbai (pp. 79-82).

Ramasubbarao, G. and Sankar, S.G., 2013. Predicting soaked CBR value of fine grained soils using index and compaction characteristics. Jordan Journal of Civil Engineering, 7(3), pp.354-360.

Reddy S., C.N.V., and Pavani, K. (2006). Mechanically stabilized soils-regression equation for CBR evaluation. In: Proceedings of Indian Geotechnical Conference, Chennai, India. Dec. 14–16, pp. 731–734.

Rehman, A.U., Farooq, K. and Mujtaba, H., 2017. Prediction of California bearing ratio (CBR) and compaction characteristics of granular soils. Acta Geotechnica Slovenica, 14(1), pp.63-72.

Saikia, A., Baruah, D., Das, K., Rabha, H.J., Dutta, A. and Saharia, A., 2017. Predicting compaction characteristics of fine-grained soils in terms of Atterberg limits. International Journal of Geosynthetics and Ground Engineering, 3(2), pp.1-9.

Shams, M.A., Shahin, M.A. and Ismail, M.A., 2020. Design of Stiffened Slab Foundations on Reactive Soils Using 3D Numerical Modeling. International Journal of Geomechanics, 20(7), p.04020097.

Sivrikaya, O., Togrol, E. and Kayadelen, C., 2008. Estimating compaction behavior of fine-grained soils based on compaction energy. Canadian Geotechnical Journal, 45(6), pp.877-887.

Sridharan, A. and Nagaraj, H.B., 2005. Plastic limit and compaction characteristics of finegrained soils. Proceedings of the institution of civil engineers-ground improvement, 9(1), pp.17-22.

Talukdar, D.K., 2014. A study of correlation between California Bearing Ratio (CBR) value with other properties of soil. International Journal of Emerging Technology and Advanced Engineering, 4(1), pp.559-562.

Tenpe, A.R. and Patel, A., 2020a. Utilization of support vector models and gene expression programming for soil strength modeling. Arabian Journal for Science and Engineering, 45, pp.4301-4319.

Tenpe, A.R. and Patel, A., 2020b. Application of genetic expression programming and artificial neural network for prediction of CBR. Road Materials and Pavement Design, 21(5), pp.1183-1200.

Venkatasubramanian, C. and Dhinakaran, G., 2011. ANN model for predicting CBR from index properties of soils. International Journal of Civil and Structural Engineering, 2(2), pp.614-620.

Vinod, P. and Reena, C., 2008. Prediction of CBR value of lateritic soils using liquid limit and gradation characteristics data. Highway Research Journal, IRC, 1(1), pp.89-98.

Wang, B., Moayedi, H., Nguyen, H., Foong, L.K. and Rashid, A.S.A., 2019. Feasibility of a novel predictive technique based on artificial neural network optimized with particle swarm optimization estimating pullout bearing capacity of helical piles. Engineering with Computers, DOI: https://doi.org/10.1007/s00366-019-00764-7

Wang, H., Moayedi, H. and Foong, L.K., 2020. Genetic algorithm hybridized with multilayer perceptron to have an economical slope stability design. Engineering with Computers, DOI: https://doi.org/10.1007/s00366-020-00957-5

Wang, H.L., Yin, Z.Y., Zhang, P. and Jin, Y.F., 2020. Straightforward prediction for air-entry value of compacted soils using machine learning algorithms. Engineering Geology, 105911.

Yildirim, B. and Gunaydin, O., 2011. Estimation of California bearing ratio by using soft computing systems. Expert Systems with Applications, 38(5), pp.6381-6391.

Zhang, W. and Goh, A.T., 2016. Multivariate adaptive regression splines and neural network correlations for prediction of pile drivability. Geoscience Frontiers, 7(1), pp.45-52.

Zhang, W., Zhang, R., Wu, C., Goh, A.T.C., Lacasse, S., Liu, Z. and Liu, H., 2020. State-of-the-art review of soft computing applications in underground excavations. Geoscience Frontiers, 11(4), pp.1095-1106.